

# Controlling Charge States of Large Ions

Mark Scalf, Michael S. Westphall, Joern Krause,\*  
Stanley L. Kaufman,† Lloyd M. Smith‡

The charge state of ions produced in electrospray ionization (ESI) was reduced in a controlled manner to yield predominantly singly charged species by exposure of the aerosol to a bipolar ionizing gas. Analysis of the resulting ions on an orthogonal time-of-flight mass spectrometer yielded mass spectra greatly simplified compared with conventional ESI spectra. The decreased spectral complexity afforded by the charge reduction facilitates the analysis of mixtures by ESI mass spectrometry.

The techniques of ESI (1) and matrix-assisted laser desorption/ionization (MALDI) (2) produce gas-phase ions of biomolecules for their analysis by mass spectrometry (MS). ESI and MALDI differ in a number of respects, including the complexity of the mass spectra produced: ESI produces a distribution of ions in various charge states, and correspondingly complex mass spectra, whereas MALDI yields predominantly singly charged ions and correspondingly simple mass spectra. This difference makes ESI generally unsuitable for the analysis of mixtures because of excessive overlap in the spectral features from the various components, in contrast to MALDI which is well suited for such analyses. MALDI, however, is less gentle and typically provides lower resolution of high-mass ions than does ESI (3).

In both MALDI and ESI desorption and ionization are closely intertwined, and it has not generally been possible to control the two processes independently. In ESI, buffer containing the analyte is passed through a capillary orifice maintained at a high electric potential. A stream of charged droplets is formed and subsequent desolvation leads eventually to a stream of charged ions. Previous work has explored the potential for charge reduction to simplify ESI mass spectra of large molecules. Several studies have shown that charge state complexity can be reduced by gas-phase reactions using merged gas streams containing oppositely charged species (4), by varying solution conditions (5), or by gas-phase ion-ion reactions in a quadrupole ion trap (6–8).

We describe here an approach that permits the charge state of ions generated in an electrospray plume to be reduced in a controlled manner, and for the resultant ions to be ana-

lyzed in an orthogonal time-of-flight (TOF) mass spectrometer (9). Charge reduction is achieved by exposure of the electrospray-generated aerosol to a neutralizing gas containing a high concentration of bipolar (that is, both positively and negatively charged) ions (10). Collisions between the charged aerosol and the bipolar ions present in the bath gas result in neutralization of the multiply charged electrospray ions (11). The rate of this process may be controlled by varying the concentration of bipolar ions in the bath gas, which in turn is controlled by the degree of exposure to a  $^{210}\text{Po}$   $\alpha$  ionization source. This provides, in effect, the ability to “tune” the charge state of the electrospray-generated ions. A practical consequence is the ability to manipulate the charge distribution on electrospray-generated ions such that it consists principally of singly charged ions and neutrals, simplifying the mass spectra and thereby facilitating the analysis of mixtures.

The instrument has three basic components: a positive-pressure ESI source (12), a charge neutralization chamber (Fig. 1), and an orthogonal TOF mass spectrometer. The electrospray-generated aerosol containing analyte is swept into the neutralization chamber by a flow of medical air bath gas (4 liters/min). The neutralization chamber is cylindrical with a diameter of 1.9 cm and a length of 4.3 cm. The gas is ionized by exposure to a 5-mCi  $^{210}\text{Po}$   $\alpha$  particle source, and reactions between the resultant ions and the aerosol droplets or analyte ions leads to neutralization (13). Two factors are important in determining the degree of charge neutralization occurring in the chamber: the  $\alpha$  particle flux from the radioactive source and the residence time of the aerosol particles in the neutralization chamber. The  $\alpha$  particle flux is readily controlled by placing thin brass disks with various numbers of holes punched in them between the  $^{210}\text{Po}$  source and the neutralization chamber; the source is completely shielded by a brass disk with no holes and shielded proportionally to the exposed surface area when holes are present in the disks. The residence time of the aerosol particles is

- (Memoires et Travaux du Centre de Recherche Français de Jerusalem, Association Paléorient, Paris, 1987), pp. 115–150].
- A. M. Radmilli, *Gli Scavi Nella Grotta Polesini a Ponte Lucano di Tivoli e la Piu Antica Arte nel Lazio* (Sansoni Editore, Firenze, 1974).
  - P. Cassoli, *Quaternaria* **19**, 187 (1976/77).
  - S. L. Kuhn et al., *Report on the 1997 Excavation Season at Meged Rockshelter (Upper Galilee, Israel)*, Permit G-47/97 (Report to Israel Antiquities Authority, Jerusalem, 1998).
  - O. Bar-Yosef et al., *Curr. Anthropol.* **33**, 497 (1992); O. Bar-Yosef et al., *J. Archaeol. Sci.* **23**, 297 (1996).
  - N. J. Shackleton and N. D. Opdyke, *Quat. Res.* **3**, 39 (1973); S. Bottema, in *Chronologies in the Near East*, G. Aurenche, J. Ervin, P. Hours, Eds. (Bar International Series, Oxford, 1987), pp. 295–310; E. Tchernov, *Paléorient* **23**, 209 (1998).
  - S. Botkin, in *Modeling Change in Prehistoric Subsistence Economies*, T. K. Earle and A. L. Christenson, Eds. (Academic Press, New York, 1980), pp. 121–139.
  - G. A. Clark and L. G. Straus, in *Hunter-Gatherer Economy in Prehistory*, G. Bailey, Ed. (Cambridge Univ. Press, Cambridge, 1983), pp. 131–148; R. G. Klein, *The Human Career: Human Biological and Cultural Origins* (Univ. of Chicago Press, Chicago, 1989).
  - M. C. Stiner, *Curr. Anthropol.* **33**, 433 (1992).
  - C. Gamble, *The Palaeolithic Settlement of Europe* (Cambridge Univ. Press, Cambridge, 1986); M. C. Stiner, *Quat. Nova* **1**, 333 (1990/91).
  - W. H. Oswalt, *An Anthropological Analysis of Food-Getting Technology* (Wiley, New York, 1976).
  - J. H. Steward, *Basin-Plateau Aboriginal Sociopolitical Groups* (Bulletin No. 120, Bureau of American Ethnology, Washington, DC, 1938).
  - S. L. Kuhn and M. C. Stiner, in *Creativity in Human Evolution and Prehistory*, S. Mithen, Ed. (Routledge, London, 1998), pp. 143–164.
  - Following Stephens and Krebs [D. W. Stephens and J. R. Krebs, *Foraging Theory* (Princeton Univ. Press, Princeton, NJ, 1986)].
  - K. V. Flannery, in *The Domestication and Exploitation of Plants and Animals*, P. J. Ucko and G. W. Dimbleby, Eds. (Aldine, Chicago, 1969), pp. 73–100; L. R. Binford, in *New Perspectives in Archaeology*, S. R. Binford and L. R. Binford, Eds. (Aldine, Chicago, 1968), pp. 313–341; M. N. Cohen, *The Food Crisis in Prehistory: Overpopulation and the Origins of Agriculture* (Yale Univ. Press, New Haven, CT, 1977); O. Bar-Yosef and A. Belfer-Cohen, *J. World Prehistory* **3**, 447 (1989); L. H. Keeley, in *Last Hunters—First Farmers*, T. D. Price and A. B. Gebauer, Eds. (School of American Research, Santa Fe, NM, 1995), pp. 243–272; P. J. Watson, in *ibid.*, pp. 21–37.
  - Compare recent studies by D. O. Henry [From *Foraging to Agriculture: The Levant at the End of the Ice Age* (Univ. of Pennsylvania Press, Philadelphia, 1989)], P. C. Edwards [Antiquity **63**, 225 (1989)], and M. P. Neeley and G. A. Clark [in *Hunting and Animal Exploitation in the Later Palaeolithic and Mesolithic of Eurasia*, G. L. Peterkin, H. Bricker, P. Mellars, Eds. (Archaeological Papers of the American Anthropological Association, Washington, DC, 1993), vol. 4, pp. 221–240].
  - See, for example, J. C. Long, *Annu. Rev. Anthropol.* **22**, 251 (1993); S. Sherry et al., *Hum. Biol.* **66**, 761 (1994); D. E. Reich and D. B. Goldstein, *Proc. Natl. Acad. Sci. U.S.A.* **95**, 8119 (1998).
  - Supported by grants from the National Science Foundation (SBR-9511894 to M.C.S. and SBR-9409281 to O.B.-Y.) and the Levi-Sala (Care) Archaeological Foundation (to N.D.M.). We thank S. L. Kuhn for advice on simulation model development, unpublished data on Meged Rockshelter, and assistance in manuscript preparation. Thanks also to A. Belfer-Cohen, A. Segre, E. Segre-Naldini, A. Bietti, and P. Cassoli for access to and information on the faunal collections from Israel and Italy; to A. Recchi for unpublished data on bird remains from Riparo Mochi; to S. Heppel, Y. Werner, and J. Behler for information on Mediterranean tortoise ecology; and to H. Harpending and anonymous reviewers for many helpful comments on this manuscript.

25 September 1998; accepted 24 November 1998

Department of Chemistry, University of Wisconsin, Madison, WI 53706–1396, USA.

\*Present address: Winkelstrasse 25, 4665 Oftringen, Switzerland.

†Present address: TSI, Inc., P.O. Box 64394, St. Paul, MN 55164, USA.

‡To whom correspondence should be addressed.

controlled by varying the flow rate of the bath gas. By balancing the residence time with the  $\alpha$  particle source exposure, one can obtain a charge distribution characteristic of a "neutral" aerosol (10).

The neutralized aerosol exits the neutralization chamber through a 3-mm-diameter outlet held at the same potential as the entrance nozzle of the mass spectrometer. A portion of the aerosol is swept into the entrance nozzle of the spectrometer. An orthogonal TOF mass spectrometer (PerSeptive Biosystems Mariner Biospectrometry Workstation) was chosen for these studies on the basis of the greater mass-to-charge ratio ( $m/z$ ) range accessible with this instrument configuration than with other mass analyzer designs. The Mariner spectrometer has a  $m/z$  range of 25,000 atomic mass units (amu) with a measured external mass accuracy of better than 100 ppm. The original electrospray chamber of the instrument was replaced with the ESI source and neutralization chamber described above.

A series of positive ion mass spectra was obtained in the analysis of the protein ubiquitin (8564.8 amu) at increasing levels of exposure to the  $^{210}\text{Po}$   $\alpha$  particle source. With the  $^{210}\text{Po}$  source completely shielded (Fig. 2A), a typical ESI charge distribution was observed, with six major charge states evident (+7 to +2) and with the peak of the distribution corresponding to the +5 charge state. As the degree of exposure to the  $^{210}\text{Po}$  source was increased (Fig. 2B), the charge

state distribution moved toward lower and fewer charge states, until with the source completely unshielded (Fig. 2C), only two major charge states were observed, with the

major peak corresponding to the +1 charge state. This result demonstrates the ability to control the charge state by varying exposure to the ionizing source.

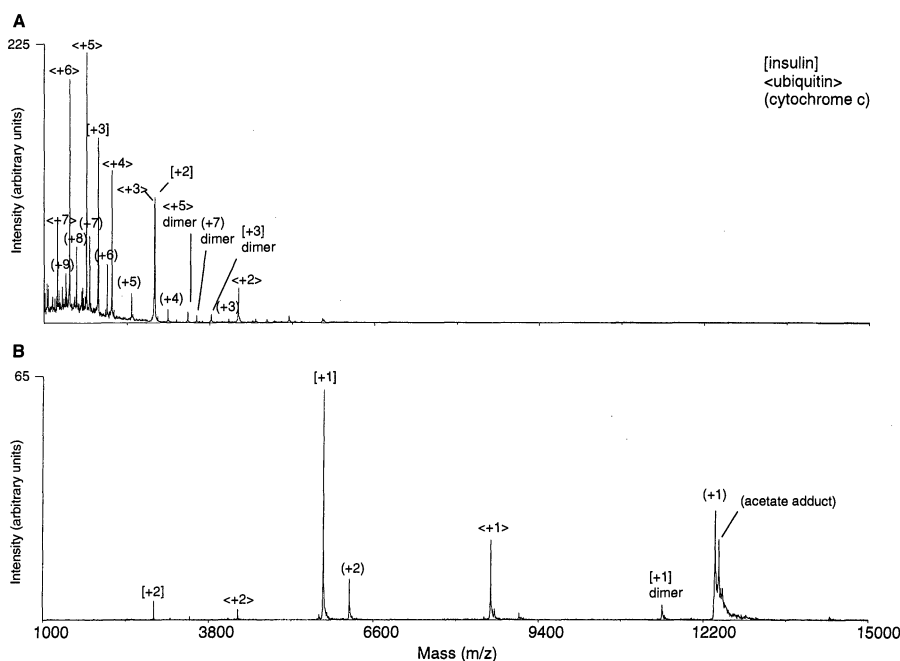


**Fig. 3.** Mixture of insulin, ubiquitin, and cytochrome c ( $5 \mu\text{M}$  each in 1:1  $\text{H}_2\text{O}$ :acetonitrile, 1% acetic acid) mass analyzed (A) without charge reduction and (B) with charge reduction. The absence of the acetate adduct on the +2 charge state of cytochrome c can be attributed to CAD in the nozzle-skimmer region. The averaged mass spectra shown were obtained over a 250-s time period at a spectral acquisition rate of 10 kHz, consuming  $0.54 \mu\text{l}$  ( $2.7 \text{ pmol}$ ) of sample. The spectra were smoothed by convolution with a Gaussian function included in the software supplied with the spectrometer.

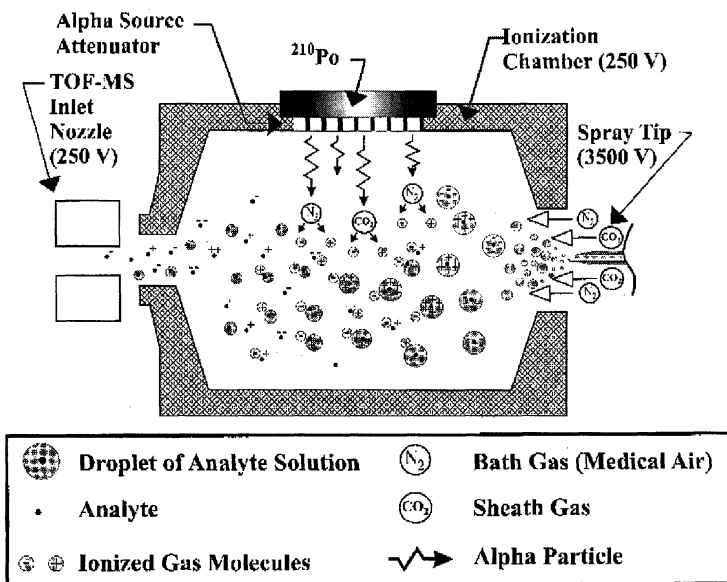
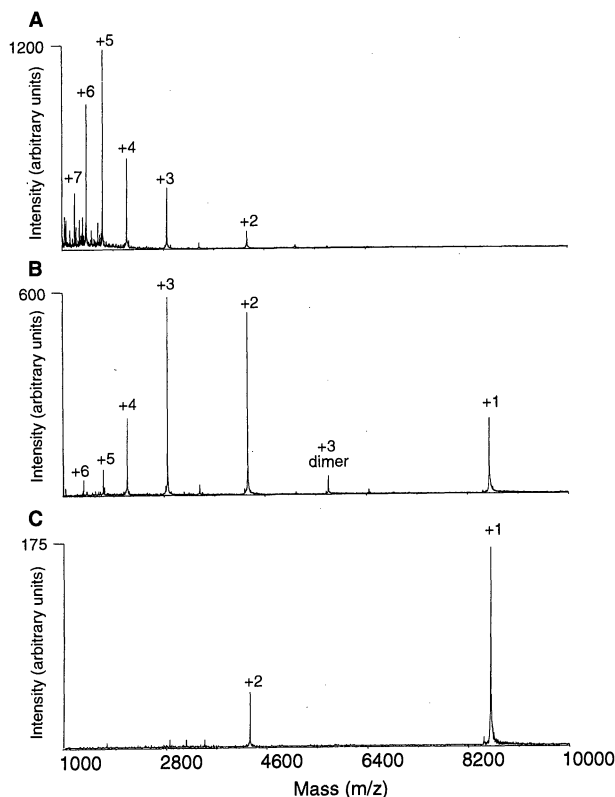


**Fig. 1 (left).** Schematic diagram of the charge neutralization apparatus. **Fig. 2 (right).** Charge-state reduction of ubiquitin ( $5 \mu\text{M}$  in 1:1  $\text{H}_2\text{O}$ :acetonitrile, 1% acetic acid) as a function of exposed area of the  $^{210}\text{Po}$   $\alpha$  particle source: (A) control (0% exposed), (B) 17.5%, and (C) 100%. The averaged mass spectra shown were obtained over a 250-s time period at a spectral acquisition rate of 10 kHz, consuming  $0.54 \mu\text{l}$  ( $2.7 \text{ pmol}$ ) of sample.



The effect of charge reduction on the analysis of a simple protein mixture by ESI is shown in Fig. 3. An equimolar mixture of three proteins (insulin, 5733.5 amu; ubiquitin, 8564.8 amu; and cytochrome c, 12,360 amu) was prepared and mass analyzed with and without charge reduction. The result obtained in the absence of charge reduction (Fig. 3A) corresponds to a fairly typical ESI mass spectrum for such a mixture (7). The mass spectrum is complex, containing about 50 peaks, 18 of which correspond to various charge states of the proteins as shown in the figure. In contrast, the spectrum shown in Fig. 3B exhibits only eight major peaks, which are readily assigned as shown. This result demonstrates the reduction of spectral complexity in mixture analysis afforded by charge reduction.

The effect of charge reduction on the analysis of a simple oligonucleotide mixture by ESI is shown in Fig. 4. An equimolar mixture of three oligonucleotides 15, 21, and 27 nucleotides in length was prepared and mass analyzed with and without charge reduction. In the absence of charge reduction ( $^{210}\text{Po}$  source shielded, Fig. 4A) a complex mass spectrum was obtained, with peaks corresponding to several different charge states for the three oligonucleotides in the mixture, as well as many other peaks due to fragmenta-

tion (see below). Charge reduction (Fig. 4B) greatly simplified the mass spectrum, with only six major peaks evident, corresponding to the singly and doubly charged ions for each oligonucleotide.

All of the unreduced charge spectra (Figs. 2A, 3A, and 4A) show a number of peaks in the low  $m/z$  region that do not correspond to charge states of the analytes and that disappear in the charge-reduced spectra. The  $m/z$  ratios and isotopic distributions of these peaks correspond predominantly to singly charged fragment ions, with a few multiply charged fragment ions as well (assignments not shown). The disappearance of these peaks with charge reduction is advantageous in a practical sense because it constitutes a substantial reduction in the "chemical noise" of the system. The observed results are consistent with the occurrence of collision-activated dissociation (CAD) in the nozzle-skimmer region of the mass spectrometer (14). Multiply charged ions are more prone to such dissociation reactions (15); by decreasing the ion charge, charge reduction will thus tend to reduce such fragmentation.

The signal intensities in the charge-reduced spectra were substantially lower than those in the unreduced spectra, which is expected because the charge reduction process converts ions to neutral species that are not

detected (10). Conversely, the reduction in chemical noise described above and simplification of the spectra both tend to increase detection sensitivity. More study will be needed to determine the trade-offs in these factors and to quantitatively assess the change in detectability that is associated with charge reduction. The mass resolutions of the spectra are unaffected by the charge reduction process, with typical resolutions of about 1000 with or without charge reduction.

Previous approaches to charge reduction in ESI fall into two major categories: modification of the solution conditions [for example, buffer, pH, salts (5)] or utilization of gas-phase reactions within an ion trap spectrometer (6–8). Both the approach described here and the ion trap studies decouple the ion production process from the neutralization process: this is important because it provides flexibility with respect to the electrospray conditions, which is critical to obtaining high-quality results, and also permits control of the degree of charge neutralization. The approach presented here has further advantages compared with the previous ion trap studies; most importantly, the cation or anion used for charge reduction does not have to be "trapped" with the electrospray ions. This has the practical consequence of permitting charge reduction to be performed on virtually any  $m/z$  range of ions, independent of the neutralizing cation or anion's  $m/z$  value; in contrast, the restricted  $m/z$  window characteristic of ion traps limits the analyte  $m/z$  range accessible with a given neutralizing ion (8). In addition, because a specific anionic or cationic species is not required, switching between positive and negative modes of electrospray is straightforward. This allows proteins to be neutralized in positive ion mode (Fig. 3), or DNA anions to be neutralized in negative ion mode (Fig. 4), without having to change any instrumental conditions other than the operating polarity. Lastly, this approach is readily implemented by a simple modification of the ESI source and is thus adaptable to virtually any mass analyzer.

The reduction of charge state described above necessarily increases the  $m/z$  ratio of the ions being analyzed. In conventional ESI-MS, even very large molecules [for example, megadaltons in size (16)] are produced with  $m/z$  ratios below 10,000, enabling their analysis with a variety of mass analyzer designs. However, with charge reduction the relatively high mass of common proteins and nucleic acids can quickly exceed the  $m/z$  range accessible with most instruments. An orthogonal-TOF system such as the one used here is clearly the best design presently available for such applications because of the very high intrinsic  $m/z$  range of TOF analysis. However, the particular instrument we used is limited by timing and other considerations to a

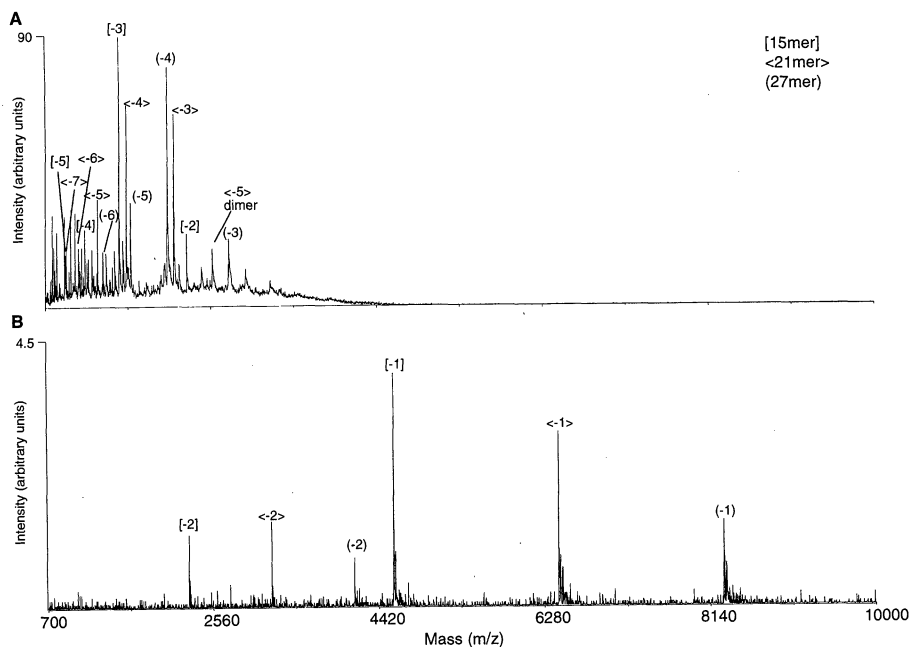


**Fig. 4.** Mixture of three oligonucleotides, a 15-nucleotide oligomer d(TGTAACGACGGCC), a 21-nucleotide oligomer d(TGTAACGACGGCCAGTGCC), and a 27-nucleotide oligomer d(TGTAACGACGGCCAGTGCCAAGCTT), mass analyzed (A) without charge reduction and (B) with charge reduction. Each oligonucleotide was at a concentration of 10  $\mu\text{M}$  in 3:1  $\text{H}_2\text{O}:\text{CH}_3\text{OH}$ , 400 mM 1,1,1,3,3,3-hexafluoro-2-propanol (HFIP) [adjusted to pH 7 with triethylamine (17)]. The HFIP buffer was found to yield the least  $\text{Na}^+$  and  $\text{K}^+$  oligonucleotide adduction of any buffer tested and was used for that reason. The averaged mass spectra shown were obtained over a 500-s time period at a spectral acquisition rate of 10 kHz, consuming 1.08  $\mu\text{l}$  (5.4 pmol) of sample. The spectra were smoothed by convolution with a Gaussian function included in the software supplied with the spectrometer.

*m/z* range below 25,000. The design and development of a mass analyzer better suited for this method of ion generation is an important area for future work.

References and Notes

1. J. B. Fenn, M. Mann, C. K. Meng, S. F. Wong, C. M. Whitehouse, *Science* **246**, 64 (1989).
2. M. Karas and F. Hillenkamp, *Anal. Chem.* **60**, 2299 (1988); F. Hillenkamp, M. Karas, R. Beavis, B. Chait, *ibid.* **63**, 1193 (1991).
3. J. B. Fenn, M. Mann, C. K. Meng, S. F. Wong, C. M. Whitehouse, *Mass Spectrom. Rev.* **9**, 37 (1990).
4. R. R. Ogorzalek-Loo, H. R. Udseth, R. D. Smith, *J. Phys. Chem.* **95**, 6412 (1991); *J. Am. Soc. Mass Spectrom.* **3**, 695 (1992).
5. U. Mirza and B. Chait, *Anal. Chem.* **66**, 2898 (1994); X. Cheng, D. C. Gale, R. D. Smith, *ibid.* **67**, 586 (1995); D. C. Muddiman, X. Cheng, H. R. Udseth, R. D. Smith, *J. Am. Soc. Mass Spectrom.* **7**, 697 (1996).
6. J. L. Stephenson Jr. and S. A. McLuckey, *J. Am. Chem. Soc.* **118**, 7390 (1996); J. L. Stephenson Jr., G. J. Van Berkel, S. A. McLuckey, *J. Am. Soc. Mass Spectrom.* **8**, 637 (1997); J. L. Stephenson Jr. and S. A. McLuckey, *Rapid Commun. Mass Spectrom.* **11**, 875 (1997); *Anal. Chem.* **70**, 1198 (1998); *J. Am. Soc. Mass Spectrom.* **9**, 957 (1998); *J. Mass Spectrom.* **33**, 664 (1998); *Anal. Chem.* **70**, 3533 (1998).
7. J. L. Stephenson Jr. and S. A. McLuckey, *J. Am. Soc. Mass Spectrom.* **68**, 4026 (1996).
8. ———, *Int. J. Mass Spectrom.* **165**, 419 (1997); *J. Am. Soc. Mass Spectrom.* **9**, 585 (1998).
9. J. H. J. Dawson and M. Guilhaus, *Rapid Commun. Mass Spectrom.* **3**, 155 (1989); J. G. Boyle and C. M. Whitehouse, *Anal. Chem.* **64**, 2084 (1992); O. A. Mirgorodskaya, A. A. Shevchenko, I. V. Chernushevich, A. F. Dodonov, A. I. Miroshnik, *ibid.* **66**, 99 (1994); A. N. Verentchikov, W. Ens, K. G. Standing, *ibid.*, p. 126; A. N. Krutchinsky, I. V. Chernushevich, V. L. Spicer, W. Ens, K. G. Standing, *J. Am. Soc. Mass Spectrom.* **9**, 569 (1998).
10. N. A. Fuchs, *Geofis. Pura Appl.* **56**, 185 (1963); D. W. Cooper and P. C. Reist, *J. Colloid Interface Sci.* **45**, 17 (1973); B. Y. H. Liu and D. Y. H. Pui, *ibid.* **49**, 305 (1974); F. Zarrin, S. L. Kaufman, F. D. Dorman, U.S. Patent 5 076 097 (1991); K. C. Lewis *et al.*, *Anal. Chem.* **66**, 2285 (1994); S. Mouradian *et al.*, *ibid.* **69**, 919 (1997).
11. The charge reduction process could in principle involve reactions of the bipolar neutralizing gas with either the electrospray-generated droplets or the electrospray-generated ions. This important mechanistic distinction is closely related to a controversy in the literature as to the mechanism of ion generation in ESI [M. Dole *et al.*, *J. Chem. Phys.* **49**, 2240 (1968); J. V. Iribarne and B. A. Thomson, *ibid.* **64**, 2287 (1976); B. A. Thomson and J. V. Iribarne, *ibid.* **71**, 4451 (1979); F. W. Röllgen, E. Bramer-Wegen, L. Bütfering, *J. Phys. (Paris)* **48**, C6-253 (1987); G. Schmelzeisen-Redeker, L. Bütfering, F. W. Röllgen, *Int. J. Mass Spectrom. Ion Processes* **90**, 139 (1989)], and in the present work it also relates to the question of where in the system the droplets are transformed into ions. The experiments reported here do not permit discrimination between these two mechanisms.
12. The ESI ion source consists of a 38-cm-long fused-silica capillary (150- $\mu\text{m}$  outer diameter, 25- $\mu\text{m}$  inner diameter) with the spray end conically ground to a cone angle (angle between the capillary axis and cone surface) of 35° (#2001145, Polymicro Technologies, Phoenix, AZ). The inlet of the capillary is immersed in analyte solution, and a positive pressure of 10 psi (70 kpa) is applied to the sample container to produce a typical flow rate of 0.13  $\mu\text{L}/\text{min}$ . The solution is maintained at a potential of +3500 V (proteins in positive ion mode) or -2950 V (DNA in negative ion mode) relative to the inlet of the ionization chamber by means of a platinum electrode immersed in the sample. The spray is stabilized against corona discharge [J. Zeleny, *Proc. Cambridge Philos. Soc.* **18**, 71 (1915); M. G. Ikonomou, A. T. Blades, P. Kebarle, *J. Am. Soc. Mass Spectrom.* **2**, 497 (1991)] with a

sheath gas of CO<sub>2</sub> (1 liter/min) fed through a stainless steel tube (1.5-mm inner diameter) concentric with the silica capillary. The <sup>210</sup>Po  $\alpha$  particle source was obtained from NRD Incorporated, Grand Island, NY (#P-2042).

13. S. L. Kaufman, F. Zarrin, F. D. Dorman, U.S. Patent 5 247 842 (1993); D. Chen, D. Y. H. Pui, S. L. Kaufman, *J. Aerosol Sci.* **26**, 963 (1995); S. L. Kaufman, J. W. Skogen, F. D. Dorman, F. Zarrin, *Anal. Chem.* **68**, 1895 (1996); S. L. Kaufman, in preparation.
14. R. D. Smith, J. A. Loo, C. J. Barinaga, C. G. Edmonds, H. R. Udseth, *J. Am. Soc. Mass Spectrom.* **1**, 53 (1990).
15. J. A. Loo, H. R. Udseth, R. D. Smith, *Rapid Commun. Mass Spectrom.* **2**, 207 (1988).

16. R. Chen *et al.*, *Anal. Chem.* **67**, 1159 (1995); S. D. Fuerstenau and W. H. Benner, *Rapid Commun. Mass Spectrom.* **9**, 1528 (1995).
17. A. Apffel, J. A. Chakel, S. Fischer, K. Lichtenwalter, W. S. Hancock, *Anal. Chem.* **69**, 1320 (1997).
18. The work described here has benefited from the efforts of other members of our laboratory and the University of Wisconsin Department of Chemistry over several years. We particularly acknowledge the helpful contributions of S. Mouradian, C. Hop, M. Vestling, and R. Clausen in this regard. Supported by Department of Energy grant DE-FG02-91ER61130, NIH grants R01HG00321 and R01HG001808, and NIH-GMS 5T32GMO8349 training grant (M.S.).

15 July 1998; accepted 25 November 1998

# Rapid Fluctuations in Sea Level Recorded at Huon Peninsula During the Penultimate Deglaciation

Tezer M. Esat,\*† Malcolm T. McCulloch, John Chappell, Bradley Pillans, Akio Omura

About 140,000 years ago, the breakup of large continental ice sheets initiated the Last Interglacial period. Sea level rose and peaked around 135,000 years ago about 14 meters below present levels. A record of Last Interglacial sea levels between 116,000 years to 136,000 years ago is preserved at reef VII of the uplifted coral terraces of Huon Peninsula in Papua New Guinea. However, corals from a cave situated about 90 meters below the crest of reef VII are 130,000  $\pm$  2000 years old and appear to have grown in conditions that were 6°C cooler than those at present. These observations imply a drop in sea level of 60 to 80 meters. After 130,000 years, sea level began rising again in response to the major insolation maximum at 126,000 to 128,000 years ago. The early (about 140,000 years ago) start of the penultimate deglaciation, well before the peak in insolation, is consistent with the Devils Hole chronology.

The coral reef terraces at Huon Peninsula in Papua New Guinea extend more than 80 km along the coast and have been uplifted at a rate that varies from 0.5 m per 1000 years (ky) in the northwest to nearly 4 m/ky to the southeast. The high uplift rates have exposed a record of late Quaternary interglacial and interstadial sea-level high stands (1–4). Prominent among these stands is reef structure VII, which formed when the sea level rose during the penultimate deglaciation, a period that may have lasted for more than 10,000 years at ~125,000 years before present (yr B.P.), when the climate was similar to or possibly warmer than the present climate and sea levels were 3 to 5 m higher. At Kwambu, a present-day analog of terrace VII exists with a barrier reef, a lagoon, and a fringing

reef; here, the fossil terrace VII is at a height of 225 m (Fig. 1).

During an international expedition to the Huon terraces in July through August 1992, we located a large ancient sea cave in the riser of terrace VIB [isotope stage 5b-5c, with a nominal age of 90 to 100 kiloannum (ka)] (Fig. 1, Kwangam section). It is situated ~400 m west of Kwangam River, at ~90 m below the crest of reef VII. The cave presumably formed when a younger reef grew over earlier corals that were buried in rubble. An unusually large (>1 m in diameter) *Porites* coral was found just inside the entrance, and other corals were found on the floor and walls. To highlight the discovery of such a well-preserved specimen, we named the location "Aladdin's Cave." Here, we present U-series ages of corals from Aladdin's Cave and terrace VI that, combined with stratigraphic relations to other dated samples from reef tract VII, provide information on rapid sea-level changes during the course of the penultimate deglaciation and its relation to solar insolation.

The timing and duration of the Last Inter-

T. M. Esat, M. T. McCulloch, J. Chappell, B. Pillans, Research School of Earth Sciences, Australian National University, Canberra, ACT 0200, Australia. A. Omura, Kanazawa University, Kanazawa, Ishikawa 920, Japan.

\*To whom correspondence should be addressed.  
†Present address: Department of Geology, Australian National University, Canberra, ACT 0200, Australia.